

## ORIGINAL ARTICLE

# Synthesis and study of polycyanurates based on 2-carbazol-4,6-dichloro-*s*-triazine

Shahrukh T Asundaria, Vinodchandra B Patel and Keshav C Patel

Eight polycyanurates have been synthesized by the interfacial polycondensation of 2-carbazol-4,6-dichloro-*s*-triazine with 1,7-dihydroxynaphthalene (DHN-1,7), 1,4-dihydroxyanthraquinone (DHA-1,4), ethylene glycol (EG), diethylene glycol (DEG), triethylene glycol (TEG), 1,2-propanediol (Pr-1,2), 1,4-butanediol (Bu-1,4) and 1,8-dihydroxyanthraquinone (DHA-1,8). All of the polycyanurates thus synthesized were characterized for their solubility, density, viscosity, infrared spectra, nuclear magnetic resonance spectra and thermogravimetric analysis. Chlorinated solvents were found to be good solvents for all of the polymers. The density of the polycyanurates varied from 1.186 to 1.247 gm cm<sup>-3</sup>. The intrinsic viscosity of the polycyanurates followed the sequence given below: homopolycyanurates of DHN-1,7 (HPDHN-1,7) > homopolycyanurates of DHA-1,8 (HPDHA-1,8) > homopolycyanurates of DHA-1,4 (HPDHA-1,4) > homopolycyanurates of EG (HPEG) > homopolycyanurates of DEG (HPDEG) > homopolycyanurates of TEG (HPTEG) > homopolycyanurates of Bu-1,4 (HPBu-1,4) > homopolycyanurates of Pr-1,2 (HPPr-1,2). The thermal stability of the polycyanurates increased as follows: HPTEG < HPPr-1,2 < HPDEG ≈ HPBu-1,4 < HPEG < HPDHA-1,8 < HPDHA-1,4 < HPDHN-1,7.

*Polymer Journal* (2012) 44, 401–409; doi:10.1038/pj.2011.146; published online 14 March 2012

**Keywords:** carbazole; density; polyamides; solubility; thermogravimetric analysis (TGA)

## INTRODUCTION

The use of polymers is rapidly increasing in nearly every region of the world. Research in the area of *s*-triazine derivatives, which has led to fundamental knowledge of novel polymers, has become increasingly widespread in recent years. Current research and development in this field involves studying the ways in which polymers can be modified to make them suitable for specific applications. Research is now focused on materials that are not only stable but also can be easily processed, and therefore, have a practical use.

A typical approach to research in this field is to utilize a stable ring system, such as triazine, and to search for a method to connect this ring-system nucleus with a thermally stable linkage, such as an ether linkage or an aliphatic linkage, to impart flexibility and solubility along with thermal stability. A review of the literature reveals that *s*-triazine and its derivatives have been known since 1873, but their incorporation into polymer chains was not extensively studied and utilized until the late 1950s. Nakamura *et al.*<sup>1</sup> synthesized various polycyanurates by interfacial polycondensation and studied the relationship between their chemical structure and their thermal and mechanical properties. Polymers containing an *s*-triazine ring in their main chain have certain properties, including high resistance to heat and chemical attack, good mechanical and dielectric properties and an ability to be easily processed.<sup>2</sup> In addition, they are generally infusible and insoluble. Various polycyanurates are used in structural composites with glass or carbon fibers, in casting resins and binders for miscellaneous organic and inorganic

substrates, as stabilizers for plastics or as films, fibers or lacquer components.<sup>3,4</sup>

Recently, various polyesters and polyamides based on *s*-triazine derivatives have been synthesized in our laboratory.<sup>5–8</sup> We have used 2-carbazol-4,6-dichloro-*s*-triazine (CDCT) as a monomer to explore the experimental conditions for the synthesis of polymers by an interfacial technique. The present investigation should aid in determining suitable reaction conditions, studying the effects of certain specific structural features included in the polymer backbone, investigating the kinetics of the thermal degradation of the polymers synthesized and studying the effect of the chemical structure of diols on the polymers from which they are synthesized.

## Materials

The monomer CDCT was synthesized from cyanuric chloride per the reaction scheme shown in Figure 1. Fresh double-distilled water was used for the preparation of the solutions. The chloroform (Ranbaxy, Mohali, India) was washed three times with distilled water to remove traces of alcohol and was treated with anhydrous calcium chloride for 24 h before distilling. Benzene was treated with concentrated sulfuric acid in a separating funnel to remove the traces of thiophene and then thoroughly washed with water to remove the acid. It was then treated with anhydrous calcium chloride for 24 h and finally distilled. The other solvents, such as nitrobenzene, carbon tetrachloride, petroleum ether, dimethylformamide, acetone and methanol, were laboratory reagents and used as received. Chemicals including sodium hydroxide

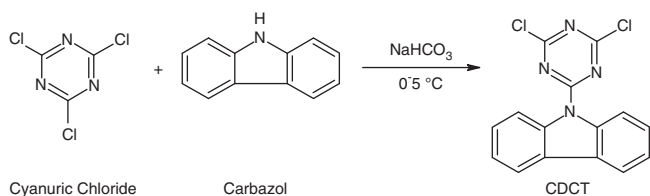


**Figure 1** Synthesis of CDCT.

pellets and sodium bicarbonate were used as received. Cyanuric chloride (Fluka, Mumbai, India) was purified by crystallization from pure benzene. Ethylene glycol (EG), diethylene glycol (DEG), triethylene glycol (TEG), 1,2-propanediol (Pr-1,2) and 1,4-butanediol (Bu-1,4) (Merck, Mumbai, India) were used as received.

### EXPERIMENTAL PROCEDURE

The polycondensation of CDCT with 1,7-dihydroxynaphthalene (DHN-1,7) has been used as a model reaction for the formation of linear aromatic polycyanurate via stirred interfacial polymerization. The formation of polycyanurate is based on the Schotten–Baumann reaction in which an acid chloride reacts with a compound containing a hydrogen atom (-OH, -NH and -SH).

#### Synthesis of the monomer

A solution of cyanuric chloride (3.69 gm, 0.02 mol) in acetone (30 ml) was added to a three-necked flask equipped with a mechanical stirrer that contained a cooled solution of sodium bicarbonate (2.12 gm) in distilled water (80 ml). This procedure resulted in the formation of a cyanuric chloride slurry. A solution of carbazole (3.34 gm, 0.02 mol) in acetone (30 ml) was slowly added to the cold slurry of cyanuric chloride. The mixture was stirred for 2 h at 0–5 °C (maintained at pH 7.0). The white product was filtered and then washed with cold water, cold dilute hydrochloric acid and finally cold water. The yield was 80% and was reduced to 75.8% after recrystallization from chloroform. The melting point was found to be 268 °C.

This reaction did not go to completion when carried out in water, unless the cyanuric chloride used was in a finely divided state. The yield of the polymer can be improved substantially if the cyanuric chloride is freshly precipitated by pouring its acetone or dioxane solution into ice water. The use of an aqueous system allows the product to be easily isolated in higher yields.<sup>9</sup>

#### Synthesis of polycyanurates

In the present investigation, all of the polycyanurates have been synthesized by an interfacial polycondensation technique with stirring.

*Synthesis of homopolycyanurates of DHN-1,7.* A mixture of DHN-1,7 (1.60 gm, 0.01 mol), sodium hydroxide (0.8 gm, 0.02 mol) and benzyl dimethyl hexadecylammonium chloride in 60 ml of double-distilled water was stirred vigorously at 25 ± 2 °C. A solution of CDCT (3.18 gm, 0.01 mol) in 30 ml of chloroform was rapidly added to the aqueous solution and the emulsion was stirred vigorously for 8 h at 25 ± 2 °C. The contents were transferred to a separating funnel and the aqueous layer was removed. The chloroform layer was washed with water and was combined with an excess of methanol from which the polymer precipitated out. The polymer was filtered and washed thoroughly with water and methanol. Approximately 76% of the theoretical yield of the polymer was obtained.

The polycyanurates of 1,4-dihydroxyanthraquinone (DHA-1,4), EG, DEG, TEG, Pr-1,2, Bu-1,4 and DHA-1,8 were synthesized under the reaction conditions optimized for the homopolymer of DHN-1,7, as shown in Figure 2.

*Synthesis of homopolycyanurates of EG.* A mixture of CDCT (3.18 gm, 0.01 mol) was heated to approximately 150 °C in a minimal quantity of dimethylformamide (10 ml). Cetrime (0.25 g) was added, followed by EG (0.62 g, 0.01 mol). The temperature was raised to 165 °C and maintained at that level for 8–10 h. The reaction mixture was cooled and poured with constant stirring into ice

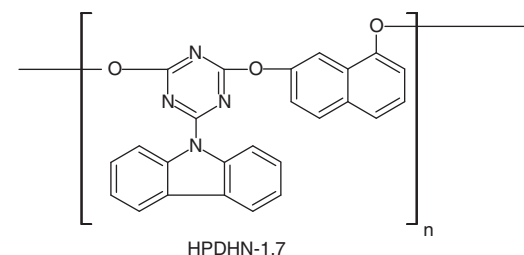
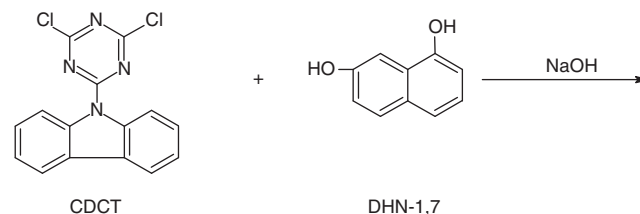


**Figure 2** Synthesis of homopolycyanurates of DHN-1,7.

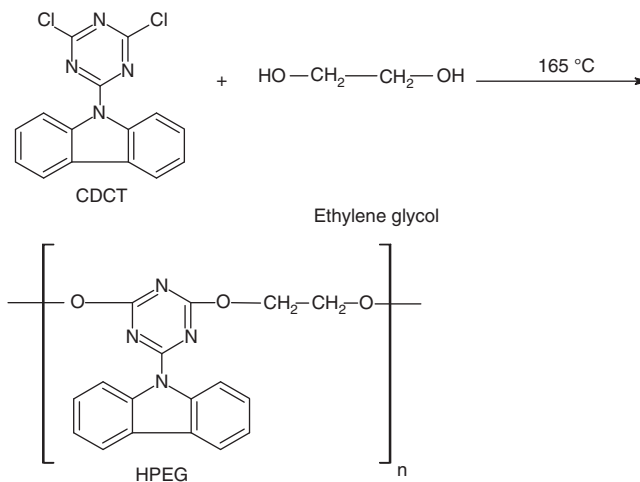


**Figure 3** Synthesis of homopolycyanurates of EG.

water. The solid was filtered, washed with hot water and then methanol, and then dried. The yield was approximately 74%.

The polycyanurates of EG, DEG, TEG, Pr-1,2, Bu-1,4 were synthesized under the reaction conditions optimized for the homopolymer of DHN-1,7, as shown in Figure 3.

#### Methods of study

The densities of the polymers were determined pycnometrically at 25 °C by the use of a suspension method, which is well suited to powdered samples.<sup>10</sup>

The infrared (IR) spectra of each polymer were recorded using a KBr disk on a Perkin-Elmer Spectrophotometer 781 (Perkin-Elmer, Thane, India). For this, AR-grade KBr was fused at red heat and was thoroughly ground. A 250-mg sample of KBr and 1.0 mg of the polymer were thoroughly mixed and ground in a mortar with glass beads. The ground mixture was then transferred to a mold and a disk was prepared by pressing it in a hydraulic press.<sup>11</sup> The disks prepared in this manner were used to obtain the IR spectra of the samples.

The viscosities of the dilute polymer solutions were conveniently measured using a Ubbelohde-type capillary viscometer.<sup>12</sup> Nuclear magnetic resonance (NMR) spectra were recorded on a Perkin-Elmer Model-32 <sup>1</sup>H-NMR Spectrometer (300 MHz) to determine the structure of the polymers.

Thermogravimetric analysis of the polymers was carried out on DuPont TA 9900 computerized thermal analyzer (Mumbai, India). This system is comprised of the TC 10A TA processor, a control unit for the thermal analysis system TA 9900 and a TG-50 thermo balance. The TG-50 thermo balance is a microbalance (reading up to 1  $\mu\text{g}$ ) fixed on a furnace controlled by the TA processor. A covered alumina crucible was used as the sample carrier. A dried polymer sample was powdered to increase its surface area. The powder was loosely poured into the alumina crucible and was dispersed to counteract the poor thermal conductivity. All of the polymers were thermogravimetrically analyzed at a heating rate of 10  $^{\circ}\text{C}\text{min}^{-1}$ . For each of these experiments, small samples (5–10 mg) were used to minimize the thermal gradient within the sample.

## RESULTS AND DISCUSSION

In this work, the physical properties of the polycyanurates were investigated, including their yield, color, solubility, density, viscosity, temperature characteristics, IR spectral characteristics, NMR shifts and the activation energy of the thermal decomposition.

### Yield and color

The yields of the polycyanurates varied from 56 to 78% depending on the reactivity of the diol component in the polymer chain. The highest yield of 78% was obtained for homopolycyanurates of DHA-1,8 (HPDHA-1,8) and the lowest yield of 56% for homopolycyanurates of EG (HPEG).

**Table 1** Yield, color and density of copolyamides

Polymer	Yield (%)	Color	Density ( $\text{g cm}^{-3}$ )
HPDHN-1,7	76	White powdery	1.233
HPDHA-1,4	72	Reddish brown	1.244
HPEG	56	Light brown	1.186
HPDEG	59	Light brown	1.209
HPTEG	61	Light brown	1.221
HPPr-1,2	58	Light brown	1.195
HPBu-1,4	62	Light brown	1.199
HPDHA-1,8	78	Reddish brown	1.247

Abbreviations: HPBu-1,4, homopolycyanurates of 1,4-butanediol; HPDEG, homopolycyanurates of diethylene glycol; HPDHA-1,4, homopolycyanurates of 1,4-dihydroxyanthraquinone; HPDHA-1,8, homopolycyanurates of 1,8-dihydroxyanthraquinone; HPDHN-1,7, homopolycyanurates of 1,7-dihydroxynaphthalene; HPEG, homopolycyanurates of ethylene glycol; HPPr-1,2, homopolycyanurates of 1,2-propanediol; HPTEG, homopolycyanurates of triethylene glycol.

The colors of the polycyanurates synthesized were influenced by the color and stereochemistry of the diols used.

The yield and color of all the polycyanurates are summarized in Table 1.

### Density

The density of each of the eight polycyanurates was determined using a pycnometer at  $25 \pm 3$   $^{\circ}\text{C}$  by suspending the polycyanurate in a liquid mixture of carbon tetrachloride and petroleum ether. This liquid system was found to be inert with respect to the polycyanurates because they remained in a state of suspension for a prolonged time. The estimated accuracy of the density measurements is  $\pm 0.001$   $\text{g cm}^{-3}$ . The density of the polycyanurates varied from 1.186 to 1.247  $\text{g cm}^{-3}$ . The highest density was displayed by HPDHA-1,8, whereas the lowest was displayed by HPEG. The densities of the polycyanurates varied with the differing chemical properties of the diols used.

The sequence of the density of the polycyanurates is as follows:

HPEG < homopolycyanurates of Pr-1,2 (HPPr-1,2) < homopolycyanurates of Bu-1,4 (HPBu-1,4) < homopolycyanurates of DEG (HPDEG) < homopolycyanurates of TEG (HPTEG) < homopolycyanurates of DHN-1,7 (HPDHN-1,7) < homopolycyanurates of DHA-1,4 (HPDHA-1,4) < HPDHA-1,8.

The density of each polycyanurate is summarized in Table 1.

### Solubility

Solubility tests were conducted using the experimental technique described as follows:

A 30–50-mg sample of each polymer was placed into a small test tube and 1 ml of solvent was added. The mixtures were stored at 25  $^{\circ}\text{C}$  with occasional shaking. The formation of streaks during shaking indicated dissolution. The polymer samples that swelled without dissolving at 25  $^{\circ}\text{C}$  were heated to 50  $^{\circ}\text{C}$  to affect the process of dissolution. Several solvents were tested for their ability to dissolve the polymer, as solubility can provide a good deal of information about the polymer.<sup>13–15</sup> The data on the relative solubility of polycyanurates are shown in Table 2 and information is presented for aliphatic chlorinated solvents such as chloroform, methylene chloride, dichloroethane, trichloroethane, tetrachloroethane, dimethylformamide and nitrobenzene. Acetone was also found to be an effective solvent for

**Table 2** Solubility of polycyanurates in various solvents

Solvent	HPDHN-1,7	HPDHA-1,4	HPEG	HPDEG	HPTEG	HPPr-1,2	HPBu-1,4	HPDHA-1,8
Chloroform	±+	±+	++	++	++	++	++	±+
Dichloroethane	±+	±+	++	++	++	++	++	±+
Dichloromethane	±+	±+	++	++	++	++	++	±+
Trichloroethylene	±+	±+	++	++	++	++	++	±+
Tetrachloroethane	±+	±+	±+	±+	±+	++	++	±+
Dimethylformamide	++	++	++	++	++	++	++	++
Dimethyl sulfoxide	–±	–±	–±	–±	–±	–±	–±	–±
Dioxane	++	++	++	++	++	++	++	++
Nitrobenzene	++	++	++	++	++	++	++	++
Chlorobenzene	++	±+	±+	±+	±+	±+	±+	±+
Cyclohexanone	±+	±+	++	++	++	±+	±+	–±
Tetrachloroethane + Phenol (50:50%)	–	–±	±±	±±	±±	–±	–±	–±

Abbreviations: HPBu-1,4, homopolycyanurates of 1,4-butanediol; HPDEG, homopolycyanurates of diethylene glycol; HPDHA-1,4, homopolycyanurates of 1,4-dihydroxyanthraquinone; HPDHA-1,8, homopolycyanurates of 1,8-dihydroxyanthraquinone; HPDHN-1,7, homopolycyanurates of 1,7-dihydroxynaphthalene; HPEG, homopolycyanurates of ethylene glycol; HPPr-1,2, homopolycyanurates of 1,2-propanediol; HPTEG, homopolycyanurates of triethylene glycol.

The first and second symbol indicates the solubility of polymer at room temperature and 50  $^{\circ}\text{C}$ , respectively. +, soluble; –, insoluble; ±, partly soluble.

polycyanurates. Dimethyl sulfoxide was determined to be a very poor solvent for each of these polymers. A noteworthy point in this examination is that chlorinated solvents, having a solubility parameter in the range of 9.3–10.4 cal cm<sup>-3</sup>, are good solvents for each of the polymers. Among these chlorinated solvents, chloroform was found to be the best solvent. The high solubility of these polymers in chloroform is attributed to the hydrogen-bond donor characteristics of chloroform. Because the hydrogen atom in chloroform is highly acidic, it can participate in hydrogen-bonding interactions with the oxygen of the ether linkage. The polymers were insoluble in aliphatic and aromatic hydrocarbons, alcohols and aliphatic esters. The solubility of the polymers was observed to increase with increasing temperature. The polymers that were partly soluble at 25 ± 3 °C were completely dissolved at higher temperatures.

### IR spectroscopy

The IR spectra of the polycyanurates exhibited several common characteristic absorption frequencies in the region of 810 cm<sup>-1</sup> that are attributed to out-of-plane and in-plane vibrations of the *s*-triazine ring. The polycyanurates involving aromatic diols in their backbone exhibited several common characteristic bands. The bands in the region of 780–650 cm<sup>-1</sup> may be due to out-of-plane bending vibra-

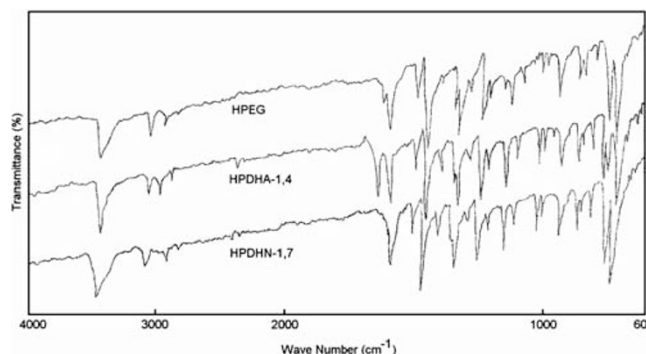


Figure 4 IR spectra of HPEG, HPDHA-1,4 and HPDHN-1,7.

tions of the C–H bonds of the aromatic rings. The bands in the 1140–980 cm<sup>-1</sup> region may be attributed to the vibration of the aryl–ether linkage and the in-plane bending vibration of the aromatic C–H in the polymers. The polycyanurates with aliphatic diols in their backbone exhibited bands in the region of 1125–970 cm<sup>-1</sup> along with the above frequencies that are assigned to the aryl–ether linkages in the polycyanurates. The frequencies in the 1260–1190 cm<sup>-1</sup> region may be attributed to vibrations involving the aryl–ether linkages.<sup>16–20</sup> Two distinct bands, observed at approximately 1330 and 1340 cm<sup>-1</sup>, respectively, along with several bands in the 1600–1590 cm<sup>-1</sup> region are attributed to the aromatic C–N stretching linkage. The bands in the region of 1490–1400 cm<sup>-1</sup> are attributed to the skeletal ring-stretching vibrations of the aromatic and heteroaromatic rings. The bands appearing in the region of 2910–2820 cm<sup>-1</sup> are assigned as saturated aliphatic C–H stretching vibrations with an absorption band at ~3060 cm<sup>-1</sup>.

It was difficult to distinguish between polycyanurates, such as HPDHN-1,7, based on frequencies in the regions of 1670–1600 and 1620–1580 cm<sup>-1</sup>, in which the ring-stretching vibrations of substituted naphthalene appear, because these regions are heavily crowded by ring-stretching vibrations of the phenyl ring. IR spectra of HPEG, HPDHA-1,4 and HPDHN-1,7 are shown in Figure 4.

The IR absorption frequencies due to various functional groups are presented in Table 3.

### NMR spectroscopy

The NMR spectra of the polycyanurates derived from CDCT and various diols indicate a multiplet band at approximately 6.80–7.93 ppm due to the presence of protons in the substituted aromatic ring system. Figure 5 shows NMR spectrum of HPDHN-1,7. The chemical shift for polycyanurate is presented in Table 4.

### Viscosity

Dilution-solution viscosity measurements were carried out using a Ubbelohde suspended-level kinematic viscometer (Cannon Instrument Co., State College, PA, USA).

Intrinsic, reduced and inherent viscosities were determined at various concentrations for each of the eight polycyanurates at

Table 3 Infrared absorption frequencies (cm<sup>-1</sup>) of polycyanurates

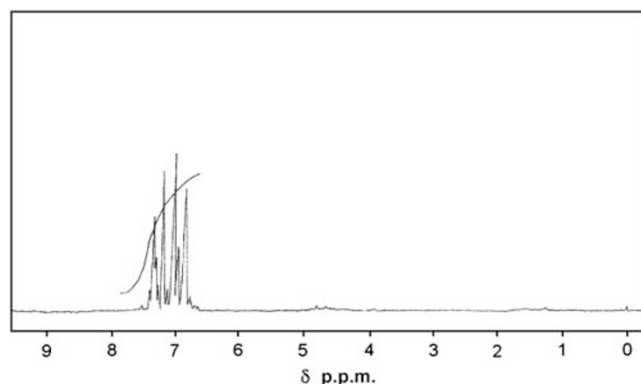
Polymers	Infrared absorption frequencies (cm <sup>-1</sup> )
HPDHN-1,7	650(w), 720(s), 780(s), 810(s), 860(s), 1000(m), 1010(s), 1110(s), 1210(s), 1230(s), 1330(s), 1600(s), 1400(m), 1450(s), 1490(s), 2820(w), 2910(s), 3020(w), 3440(vb)
HPDHA-1,4	650(w), 720(s), 760(s), 780(s), 810(s), 860(s), 980(s), 1020(m), 1080(s), 1210(s), 1230(s), 1330(s), 1590(s), 1400(m), 1450(s), 1490(s), 1630(s), 2820(w), 2910(s), 3040(w), 3100(w), 3420(vb)
HPEG	650(w), 720(s), 780(s), 810(s), 835(s), 860(s), 970(s), 1090(m), 1120(s), 1200(w), 1240(s), 1340(s), 1600(s), 1400(m), 1450(s), 1490(s), 2820(w), 2910(s), 3060(w), 3440(vb)
HPDEG	650(w), 720(s), 780(s), 810(s), 835(s), 860(s), 980(s), 1090(w), 1125(s), 1200(m), 1240(s), 1340(s), 1600(s), 1400(m), 1450(s), 1490(s), 2820(w), 2910(s), 3040(w), 3440(vb)
HPTEG	650(w), 720(s), 780(s), 810(s), 835(s), 860(s), 980(s), 1040(s), 1100(w), 1120(m), 1190(m), 1240(s), 1260(s), 1340(s), 1600(s), 1400(m), 1450(s), 1490(s), 2820(w), 2910(s), 3060(w), 3440(vb)
HPPr-1,2	650(w), 720(s), 780(s), 810(s), 835(s), 860(s), 980(s), 1040(s), 1100(w), 1120(m), 1210(m), 1250(s), 1340(s), 1600(s), 1400(m), 1450(s), 1490(s), 2820(w), 2910(s), 3060(w), 3440(vb)
HPBu-1,4	650(w), 720(s), 780(s), 810(s), 835(s), 860(s), 980(s), 1040(s), 1100(w), 1120(m), 1205(m), 1240(s), 1340(s), 1600(s), 1400(m), 1450(s), 1490(s), 2820(w), 2910(s), 3060(w), 3440(vb)
HPDHA-1,8	650(w), 720(s), 760(m), 780(s), 810(s), 860(s), 980(s), 1010(m), 1080(s), 1120(m), 1205(w), 1240(s), 1330(s), 1590(s), 1400(m), 1450(s), 1490(s), 1630(s), 2820(m), 2910(s), 3060(w), 3410(vb)

Abbreviations: HPBu-1,4, homopolycyanurates of 1,4-butanediol; HPDEG, homopolycyanurates of diethylene glycol; HPDHA-1,4, homopolycyanurates of 1,4-dihydroxyanthraquinone; HPDHA-1,8, homopolycyanurates of 1,8-dihydroxyanthraquinone; HPDHN-1,7, homopolycyanurates of 1,7-dihydroxynaphthalene; HPEG, homopolycyanurates of ethylene glycol; HPPr-1,2, homopolycyanurates of 1,2-propanediol; HPTEG, homopolycyanurates of triethylene glycol. Where (s), strong; (m), medium; (w), weak; and (vb), very broad.

**Table 4** NMR spectral characteristics of polycyanurates

Polymer	Chemical shift ( $\delta$ p.p.m.)
HPDHN-1,7	6.80–7.48 (m, Ar-H)
HPDHA-1,4	7.05–7.93 (m, Ar-H)
HPEG	4.74 (s, CH <sub>2</sub> ), 6.93–7.64 (m, Ar-H)
HPDEG	3.87 (t, CH <sub>2</sub> ), 4.46 (t, CH <sub>2</sub> ), 6.90–7.55 (m, Ar-H)
HPTEG	3.50 (s, CH <sub>2</sub> ), 3.78 (t, CH <sub>2</sub> ), 4.53 (t, CH <sub>2</sub> ), 7.18–7.74 (m, Ar-H)
HPPr-1,2	1.31 (d, CH <sub>3</sub> ), 4.12 (d, CH <sub>2</sub> ), 5.33 (m, CH), 7.22–7.70 (m, Ar-H)
HPBu-1,4	2.18 (t, CH <sub>2</sub> ), 3.76 (t, CH <sub>2</sub> ), 7.12–7.63 (m, Ar-H)
HPDHA-1,8	6.93–7.57 (m, Ar-H)

Abbreviations: HPBu-1,4, homopolycyanurates of 1,4-butanediol; HPDEG, homopolycyanurates of diethylene glycol; HPDHA-1,4, homopolycyanurates of 1,4-dihydroxyanthraquinone; HPDHA-1,8, homopolycyanurates of 1,8-dihydroxyanthraquinone; HPDHN-1,7, homopolycyanurates of 1,7-dihydroxynaphthalene; HPEG, homopolycyanurates of ethylene glycol; HPPr-1,2, homopolycyanurates of 1,2-propanediol; HPTEG, homopolycyanurates of triethylene glycol; NMR, nuclear magnetic resonance.


**Figure 5** NMR spectrum of HPDHN-1,7.

25 ± 0.1 °C. The reduced and inherent viscosities were calculated from experimental data. Typical Huggins and Kraemer plots were used to obtain the intrinsic viscosity for each of the polycyanurates. The solution viscosities of HPDHN-1,7 at different concentrations are shown in Table 5.

Intrinsic viscosity, reduced viscosity and inherent viscosity, along with Huggin's and Kraemer's constants for a 1% solution for each of the polycyanurates are shown in Table 6.

Examination of the intrinsic viscosities of the polycyanurates reveals that HPDHN-1,7 has the highest solution viscosity, and thus the highest molecular weight among all of the polycyanurates, whereas the HPPr-1,2 has the lowest solution viscosity, as shown in Figure 6. The intrinsic viscosity of the polycyanurates follows the sequence given below:

HPDHN-1,7 > HPDHA-1,8 > HPDHA-1,4 > HPEG > HPEG > HPDEG > HPTEG > HPBu-1,4 > HPPr-1,2.

This order may be attributed to the basicity strength of the diols. Thus, the reactivity towards a nucleophilic substitution reaction is higher for a less acidic diol. DHN-1,7 is less acidic, therefore, it is the most reactive among the diols used in the present investigation. In contrast, Pr-1,2 is highly acidic, thus, it is a less reactive diol. The reduced viscosity values may also be reflected in the order of reactivity with respect to the nucleophilic substitution reactions of these diols.

#### Thermal decomposition characteristics

Thermal stability is the most desirable property of a polymer. If the thermal stability of a polymer is increased, it is accompanied by an increase in its strength modules, rigidity and softening temperature. The thermal degradation reaction of a specific polymer depends upon a large number of variables, including the decomposition temperature, heating rate, rate of removal of volatile products from the reaction

**Table 5** Solution viscosity of polycyanurate of DHN-1,7 (HPDHN-1,7)

Solvent: chloroform					
Temperature: 25 °C					
Conc. (C) g dl <sup>-1</sup>	Flow time t sec	$\eta_{rel}=t/t_0$	$\eta_{sp}=\eta_{rel}-1$	Reduced viscosity ( $\eta_{sp}/C$ )	$\ln \eta_{rel}/C$
0.2	100.6	1.1055	0.1055	0.5275	0.5015
0.4	110.8	1.2176	0.2176	0.5440	0.4945
0.6	121.5	1.3352	0.3352	0.5586	0.4922
0.8	132.5	1.4560	0.4560	0.5700	0.4696
1.0	144.5	1.5879	0.5879	0.5879	0.4624

**Table 6** Various viscosity values and constants of Huggins and Kraemer equation for polycyanurates

Polymer	Intrinsic viscosity $\eta$	Reduced viscosity $\eta_{sp}/C$ (dl g <sup>-1</sup> )	Inherent viscosity ( $\ln \eta_{rel}/C$ )	Huggins constant (K)	Kraemer constant ( $\beta$ )
HPDHN-1,7	0.5125	0.5879	0.4624	0.2871	0.1905
HPDHA-1,4	0.4450	0.5020	0.4058	0.2879	0.1980
HPEG	0.4215	0.4747	0.3850	0.2994	0.2050
HPDEG	0.3795	0.4238	0.3542	0.3076	0.1756
HPTEG	0.3550	0.3850	0.3220	0.2381	0.2619
HPPr-1,2	0.2800	0.3000	0.2610	0.2551	0.2420
HPBu-1,4	0.3180	0.3480	0.2980	0.2967	0.1978
HPDHA-1,8	0.4655	0.5181	0.4100	0.2423	0.2561

Abbreviations: HPBu-1,4, homopolycyanurates of 1,4-butanediol; HPDEG, homopolycyanurates of diethylene glycol; HPDHA-1,4, homopolycyanurates of 1,4-dihydroxyanthraquinone; HPDHA-1,8, homopolycyanurates of 1,8-dihydroxyanthraquinone; HPDHN-1,7, homopolycyanurates of 1,7-dihydroxynaphthalene; HPEG, homopolycyanurates of ethylene glycol; HPPr-1,2, homopolycyanurates of 1,2-propanediol; HPTEG, homopolycyanurates of triethylene glycol. Concentration of polymer solution is 1.0 g dl<sup>-1</sup>.

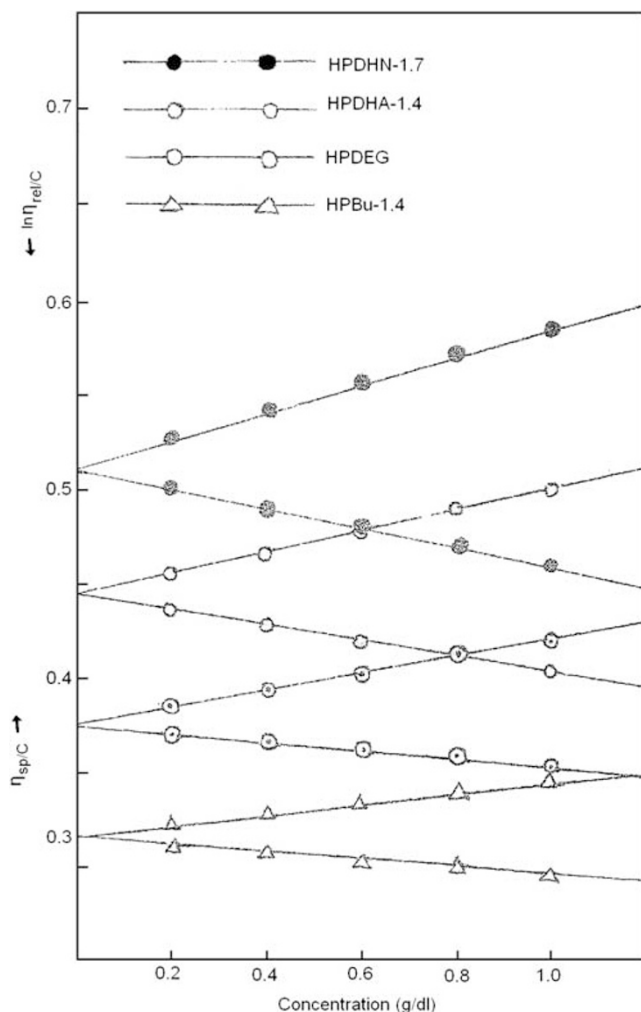


Figure 6 Huggins and Kraemer plots of intrinsic viscosity.

zone, softening and melting points of the polymer, sample size and dimension, presence of oxygen in the atmosphere or absorbed into the sample, other occluded impurities, the initiator used and the mechanism of termination in the original preparation of the polymer. Therefore, the thermal decomposition is performed under an inert atmosphere with carefully purified polymers in the form of finely divided powders.

Figure 7 shows thermogram for HPPr-1,2, HPDHA-1,4, HPDEG and HPDHN-1,7, whereas Figure 8 shows thermogram for HPDHA-1,8, HPTEG, HPEG and HPBu-1,4.

Thermogravimetric curves were obtained at a scan rate of  $10\text{ }^{\circ}\text{C min}^{-1}$  for each of the polycyanurates.

HPDHN-1,7 begins to decompose at approximately  $230\text{ }^{\circ}\text{C}$ . A slight initial weight loss below  $230\text{ }^{\circ}\text{C}$  may be due to absorbed moisture or an associated solvent. The polymer decomposes with a rapid weight loss (47.50% of its weight) in the temperature range of  $360\text{--}500\text{ }^{\circ}\text{C}$ . The maximum rate of weight loss occurs at  $440\text{ }^{\circ}\text{C}$ . Above  $530\text{ }^{\circ}\text{C}$ , the second decomposition step (having a slower rate of weight loss compared with the first step) commences with 31.50% loss of its weight. The overall decomposition leaves approximately 20.75% of residue remaining. HPDHA-1,4 exhibits two distinct stages of decomposition. The first stage occurs in the range of  $310\text{--}500\text{ }^{\circ}\text{C}$ . The maximum rate of decomposition occurs at  $400\text{ }^{\circ}\text{C}$ . The polymer

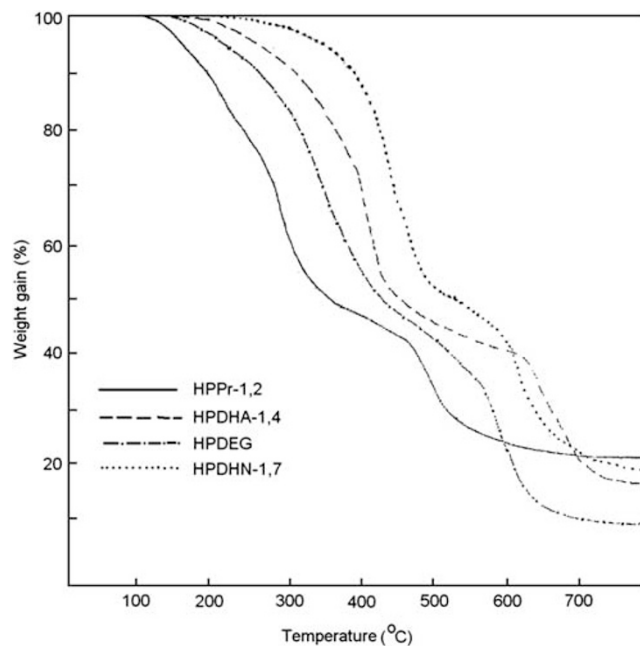


Figure 7 Thermogram for HPPr-1,2, HPDHA-1,4, HPDEG and HPDHN-1,7.

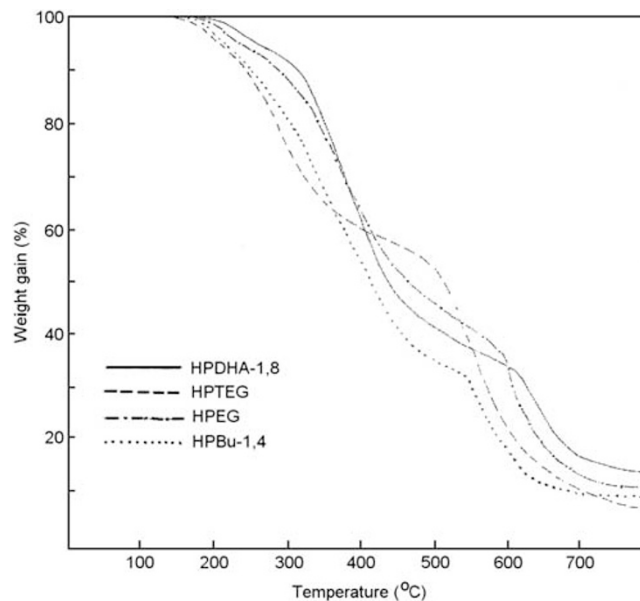


Figure 8 Thermogram for HPDHA-1,8, HPTEG, HPEG and HPBu-1,4.

loses 56.5% of its weight in this step. The second stage commences in the range of  $610\text{--}700\text{ }^{\circ}\text{C}$ . The maximum rate of decomposition occurs at  $640\text{ }^{\circ}\text{C}$ . The polymer loses 26.0% of its weight in this step and the overall decomposition ultimately leaves approximately 17.5% of the residue.

The thermogram of HPEG exhibits two distinct steps. The decomposition begins at  $\sim 170\text{ }^{\circ}\text{C}$ , with a maximum rate of decomposition at  $370\text{ }^{\circ}\text{C}$ . The polymer loses 54.50% of its weight at up to  $500\text{ }^{\circ}\text{C}$ . The second step commences at approximately  $540\text{--}700\text{ }^{\circ}\text{C}$ , during which the polymer loses 32.75% of its weight. The maximum rate of decomposition occurs at  $600\text{ }^{\circ}\text{C}$ . The overall decomposition leaves approximately 12.75% of the residue remaining.

HPDEG loses 51.0% of its weight in the temperature range of 270–440 °C with a maximum rate of decomposition at 340 °C. The second decomposition step commences in the range of 530–640 °C. The homopolymer loses 38.5% of its weight in this step.

The thermogram curves of HPTEG show two distinct steps of decomposition. The polymer begins to decompose at approximately 130 °C. The decomposition is marked with a rapid weight loss in the range of 210–380 °C, during which the polymer loses 38.0% of its weight. The maximum rate of decomposition occurs at 280 °C. The second decomposition step commences with a 53.5% loss of its weight, having a faster rate of weight loss compared with the first step. The overall decomposition leaves approximately 8.5% of its weight.

In the temperature range of 190–360 °C, HPPr-1,2 loses 51.5% of its weight. The maximum rate of weight loss occurs at 290 °C. Above 450 °C, the second decomposition step commences with loss of 26.0% of its weight and has a low rate of weight loss compared with the first step. The maximum rate of weight loss occurs at 490 °C. The decomposition ultimately leaves approximately 22.5% of the residue.

The overall degradation of HPBu-1,4 involves two steps. The first step encompasses a temperature range of 260–510 °C and involves a weight loss of approximately 63.5%. The rate of weight loss reaches a maximum at 340 °C. The second step of the degradation commences from 520–620 °C and involves a weight loss of approximately 25.0%. The maximum rate of weight loss occurs at 560 °C.

Similarly, the overall thermal degradation of HPDHA-1,8 involves two distinct steps. At a temperature of 300 °C, the first step of degradation begins and extends up to 460 °C with a weight loss of approximately 54.0%. The maximum rate of weight loss occurs at 380 °C. Above 590 °C, the second step of the decomposition commences and involves further weight loss of 31.0% at up to 700 °C with a maximum rate at 640 °C.

The characteristic temperatures for the assessment of the relative thermal stability of polycyanurates, such as the initial decomposition temperature ( $T_0$ ), temperature for 10% weight loss ( $T_{10}$ ), temperature for the maximum rate of decomposition ( $T_{max}$ ) and temperature for half volatilization ( $T_s$ ), are represented in Table 7.

The thermal stability of the polycyanurates studied was established on the basis of  $T_{max}$  for the first step of decomposition. The thermal stability of polycyanurates increases in the following order:

HPTEG < HPPr-1,2 < HPDEG  $\approx$  HPBu-1,4 < HPEG < HPDHA-1,8 < HPDHA-1,4 < HPDHN-1,7.

The thermal stability based on the half-volatilization-point temperature ( $T_s$ ) follows a somewhat different sequence. The thermal stability increases as follows:

HPPr-1,2 < HPBu-1,4 < HPDEG < HPDHA-1,4 < HPEG < HPTEG < HPDHA-1,8 < HPDHN-1,7.

The above thermal stability trends show that the polycyanurate of Pr-1,2 (HPPr-1,2) is least stable, whereas the polycyanurate of DHN-1,7 (HPDHN-1,7) possesses the highest thermal stability.

### Evaluation of the kinetic parameters

Dynamic TGA thermograms obtained at a heating rate of 10 °C min<sup>-1</sup> have been analyzed according to the graphical methods proposed by Broido, Horowitz–Metzger. Broido plot for thermal degradation of HPDHN-1,7 is depicted in Figure 9. Horowitz–Metzger plot for thermal degradation of HPDHN-1,7 is shown in Figure 10.

A typical application of Broido's method is exemplified for HPDHN-1,7 in Table 8, and the Horowitz–Metzger method is exemplified for HPDHN-1,7 in Table 9. The straight lines are due to linear regression analysis of the experimental data. The magnitude

**Table 7** Thermal characteristics of various polycyanurates

Polymer	$T_0$	$T_{10}$	$T_{max}$		$T_s$	Residue at 800 °C
			Step I	Step II		
HPDHN-1,7	230	380	440	610	525	20.75
HPDHA-1,4	190	300	400	600	450	17.50
HPEG	170	280	370	600	475	12.75
HPDEG	140	245	340	570	420	10.50
HPTEG	130	240	280	560	510	08.50
HPPr-1,2	110	200	290	490	350	22.50
HPBu-1,4	150	250	340	560	415	11.50
HPDHA-1,8	200	315	380	650	515	14.75

Abbreviations: HPBu-1,4, homopolycyanurates of 1,4-butanediol; HPDEG, homopolycyanurates of diethylene glycol; HPDHA-1,4, homopolycyanurates of 1,4-dihydroxyanthraquinone; HPDHA-1,8, homopolycyanurates of 1,8-dihydroxyanthraquinone; HPDHN-1,7, homopolycyanurates of 1,7-dihydroxynaphthalene; HPEG, homopolycyanurates of ethylene glycol; HPPr-1,2, homopolycyanurates of 1,2-propanediol; HPTEG, homopolycyanurates of triethylene glycol;  $T_0$ , initial decomposition temperature;  $T_{10}$ , temperature for 10% weight loss;  $T_{max}$ , maximum rate of decomposition temperature;  $T_s$ , temperature for 50% weight loss.

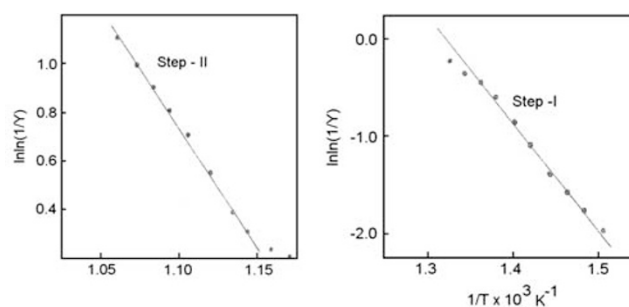


**Figure 9** Broido plot for the thermal degradation of HPDHN-1,7.

of an apparent activation energy for a degradation reaction reflects the ease with which it can proceed. Therefore, activation energy may be used to approximate the relative ease of the thermal degradation of a polymer, and hence its relative thermal stability.

The thermograms of other polymers were analyzed using the same graphical method. The values of the apparent activation energy corresponding to the different degradation steps involved were evaluated from the slopes of the least-squares plots of the relevant data and are presented in Table 10. Examination of the data indicates that both the methods yield comparable values for  $E$ . The experimental points corresponding to the initial stage (10% loss) of the thermal degradation tended to deviate from linearity. This deviation may be due to the fact that the decomposition of solids does not obey first-order kinetics in the initial stages.

Of the two methods, the Broido method is expected to provide more reliable estimates of  $E$  because no other temperature characteristics are involved.

The values for the activation energies for first step vary from 24.93 to 9.03 kcal mol<sup>-1</sup> according to the Broido method. The values for  $E$  calculated according to the Horowitz–Metzger method are in good agreement with these values. The activation energies for the second step of thermal degradation in the cases of HPEG, HPDEG, HPTEG, HPPr-1,2, HPBu-1,4 and HPDHA-1,8 are higher than those of the first step, whereas in the cases of HPDHA-1,4 and HPDHN-1,7, they are lower than those of the first step.

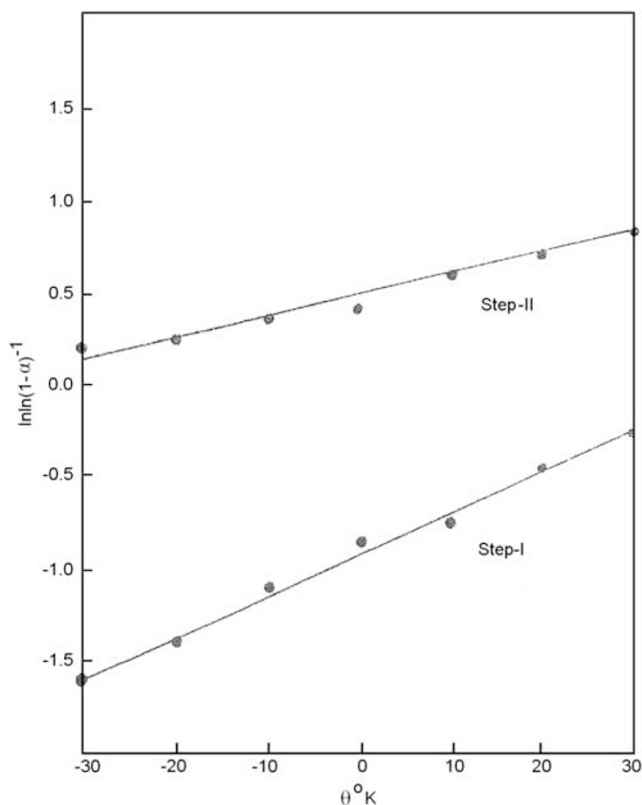


Figure 10 Horowitz-Metzger plot for the thermal degradation of HPDHN-1,7.

Table 8 Application of Broido method to thermogram of HPDHN-1,7 obtained at 10 °C/min

Temperature (°C)	% Wt	$y = \frac{W_t - W_0}{W_t - W_0}$	1/y	ln ln 1/y	T °K	1/T × 10 <sup>3</sup> °K <sup>-1</sup>
<b>Step I</b>						
390	89.50	0.8675	1.1527	-1.9510	1.5084	
400	87.50	0.8423	1.1873	-1.7623	1.4859	
410	85.50	0.8170	1.2239	-1.5991	1.4641	
420	83.00	0.7855	1.2731	-1.4211	1.4430	
430	77.00	0.7098	1.4089	-1.0706	1.4225	
440	72.50	0.6530	1.5314	-0.8529	1.4025	
450	66.00	0.5710	1.7514	-0.5791	1.3831	
460	63.00	0.5331	1.8757	-0.4636	1.3643	
470	59.00	0.4827	2.0719	-0.3168	1.3459	
480	56.50	0.4511	2.2168	-0.2281	1.3280	
<b>Step II</b>						
580	44.00	0.2934	3.4086	0.2040	1.1723	
590	43.00	0.2808	3.5618	0.2392	1.1588	
600	41.00	0.2555	3.9136	0.3108	1.1455	
610	39.00	0.2303	4.3425	0.3842	1.1325	
620	34.50	0.1735	5.7636	0.5605	1.1198	
630	31.00	0.1239	7.7317	0.7156	1.1074	
640	29.00	0.1041	9.6061	0.8164	1.0953	
650	27.50	0.0852	11.7407	0.9014	1.0834	
660	26.00	0.0662	15.0952	0.9986	1.0718	
670	24.50	0.0473	21.1333	1.1154	1.0605	

Table 9 Application of Horowitz-Metzger's method to thermogram of HPDHN-1,7 obtained at 10 °C min<sup>-1</sup>

Temperature (°C)	α	1-α	1/1-α	ln ln (1/1-α)	θ
<b>Step I</b>					
410	0.1830	0.8170	1.2239	-1.5991	-30
420	0.2145	0.7855	1.2731	-1.4211	-20
430	0.2902	0.7098	1.4089	-1.0706	-10
440	0.3470	0.6530	1.5314	-0.8529	0
450	0.4290	0.5710	1.7514	-0.5791	10
460	0.4669	0.5331	1.8757	-0.4636	20
470	0.5173	0.4827	2.0719	-0.3168	30
<b>Step II</b>					
580	0.7066	0.2934	3.4086	0.2040	-30
590	0.7192	0.2808	3.5618	0.2392	-20
600	0.7445	0.2555	3.9136	0.3108	-10
610	0.7697	0.2303	4.3425	0.3842	0
620	0.8265	0.1735	5.7636	0.5605	10
630	0.8761	0.1239	7.7317	0.7156	20
640	0.8959	0.1041	9.6061	0.8164	30

Table 10 Kinetic parameters for thermal decomposition of polycyanurates

Polymer	Energy of activation E (Kcal mol <sup>-1</sup> )			
	Broido		Horowitz-Metzger	
	Step I	Step II	Step I	Step II
HPDHN-1,7	24.93	18.54	25.66	19.27
HPDHA-1,4	16.63	12.29	16.16	12.13
HPEG	8.57	14.12	8.99	14.28
HPDEG	10.11	12.66	10.56	13.03
HPTEG	9.75	16.44	9.76	16.27
HPPr-1,2	9.03	10.68	9.30	11.99
HPBu-1,4	9.20	13.33	9.37	13.34
BPDHA-1,8	14.23	15.81	13.83	15.63

Abbreviations: HPBu-1,4, homopolycyanurates of 1,4-butanediol; HPDEG, homopolycyanurates of diethylene glycol; HPDHA-1,4, homopolycyanurates of 1,4-dihydroxyanthraquinone; HPDHA-1,8, homopolycyanurates of 1,8-dihydroxyanthraquinone; HPDHN-1,7, homopolycyanurates of 1,7-dihydroxynaphthalene; HPEG, homopolycyanurates of ethylene glycol; HPPr-1,2, homopolycyanurates of 1,2-propanediol; HPTEG, homopolycyanurates of triethylene glycol.

Examination of Table 10 reveals that HPDHN-1,7 shows the highest value of activation energy for the initial stage of thermal degradation, whereas HPEG, HPPr-1,2, HPBu-1,4, HPDEG and HPTEG show lower activation energies. Taking aromaticity into account, the polycyanurates derived from naphthalene diols are expected to be the most thermally stable among all of the polymers, but only the polycyanurate involving DHN-1,7 closely follows this assumption.

Furthermore, this trend in relative stability indicates that the initial site of degradation may lie in the nature of the bridge, 'X', in the aromatic diol component of the molecular chain. Thus, results based on the qualitative and semiquantitative treatment of the dynamic thermogravimetric data for the polymers indicate that inclusion of bisphenol-S and a symmetrical dihydroxynaphthalene moiety in the homopolymer backbone is advantageous for improved thermal stability. Moreover, such inclusion does not adversely affect the solubility of the resultant homopolymer.



## CONCLUSIONS

The properties of polycyanurates largely depend upon the structure and mode of their preparation. These properties are influenced by the nature of the substituents on the *s*-triazine nucleus and by the nature of the diol component of the polymer chain.

## ACKNOWLEDGEMENTS

We are grateful to Atul Limited, Valsad, for providing useful chemicals.

- Nakamura, Y., Mori, K., Tamura, K. & Saito, Y. Relation of the chemical structure of polycyanurates to thermal and mechanical properties. *J. Polym. Sci. A-1* **7**, 3089 (1969).
- Tigelaar, D. M., Palker, A. E., Jackson, C. M., Anderson, K. M., Wainright, J. & Savinell, R. F. Synthesis and properties of novel proton-conducting aromatic poly (ether sulfone)s that contain triazine groups. *Macromolecules* **42**, 1888–1896 (2009).
- Hamerton, I. *The chemistry and Technology of Cyanate Ester Resins* (Chapman and Hall: Glasgow, 1994).
- Ismail, V. R. M. Über triazinhaltige polytetrachlorarylester. Kurzzmitteilung. *Die. Angew. Macromol. Chem.* **21**, 25–30 (1972).
- Asundaria, S. T., Patel, P. R. & Patel, K. C. Novel copolyesters based on *s*-triazine derivatives. *Int. J. Polym. Mat.* **58**, 692–705 (2009).
- Asundaria, S. T. & Patel, K. C. Synthesis and characterization of novel copolyamides based on *s*-triazine derivatives. *Int. J. Polym. Mat.* **59**, 370–386 (2010).
- Asundaria, S. T., Patel, K. C. & Patel, H. S. Synthesis and physicochemical studies of some novel homopolyesters based on *s*-triazine. *Int. J. Polym. Mat.* **59**, 241–254 (2010).
- Patel, K. C., Asundaria, S. T. & Patel, P. R. Novel copolyamides based on *s*-triazine derivatives. *Int. J. Polym. Mat.* **59**, 118–133 (2010).
- Parsania, P. H., Shah, P. P., Patel, K. C. & Patel, R. D. Morphology property relationships in poly (2-methoxy)cyanurate of bisphenol-C (PMCBC)/polystyrene (PS) blends—dynamic modulus. *Die Angew Macromol Chem.* **138**, 139–149 (1986).
- Ashraf, S. M., Sharif, A. & Riaz, U. *A laboratory manual of polymers*. vol. 1 114 (I. K. International: New Delhi, 2009).
- Silverstein, R. M. & Webster, F. *Spectrometric Identification of Organic Compounds* 6th edn (Wiley: New York, 2005).
- Ubbelohde, L. *Ind. Eng. Chem. Anal. Edn* **9**, 85 (1935).
- Bozdogan, A. E. A method for determination of thermodynamics and solubility parameters of polymers in dilute solutions from critical volume fractions. *Polymer* **44**, 6427–6430 (2003).
- Rindfleisch, F., DiNoia, T. P. & McHugh, M. A. Solubility of polymers and copolymers in supercritical CO<sub>2</sub>. *J. Phys. Chem.* **100**, 15581–15587 (1996).
- Jang, B. N., Wang, D. & Wilkie, C. A. Relationship between the solubility parameter of polymers and the clay dispersion in polymer/clay nanocomposites and the role of the surfactant. *Macromolecules* **38**, 6533–6543 (2005).
- Choudhary, R. B., Anand, O. N. & Tyagi, O. S. Surface reactivity and layer analysis of chemisorbed reaction films in the surface-chemical environment of alkyl octadecenoates. *J. Chem. Sci.* **121**, 353–360 (2009).
- Patel, H. S. & Patel, K. C. Copolycyanurates from 2-(*N*-ethyl anilino)-4,6-bis (phenoxy-2-carbonyl chloride)-*s*-triazine: synthesis and characterization. *Iran. Polym. J.* **15**, 505–513 (2006).
- Zulfiqar, S., Ahmad, Z. & Ilyas Sarwar, M. Soluble aromatic polyamide bearing ether linkages: synthesis and characterization. *Coll. Polym. Sci.* **285**, 1749–1754 (2007).
- Yue, X., Zhang, H., Chen, W., Wang, Y., Zhang, S., Wang, G. & Jiang, G. Crosslinkable fully aromatic poly(aryl ether ketone)s bearing macrocycle of aryl ether ketone. *Polymer* **48**, 4715–4722 (2007).
- Wang, C. S. & Leu, T. S. Novel bismaleimide with naphthalene and aryl ether linkages. *J. Appl. Poly. Sci.* **73**, 833–839 (1999).